NASA

Technical Memorandum 80337

The Hard X-Ray Burst Spectrometer on the Solar Maximum Mission

L. E. Orwig, K. J. Frost and B. R. Dennis

AUGUST 1979

National Aeronautics and
Space Administration

Goddard Space Flight Center
Greenbelt, Maryland 20771

TM 80337

THE HARD X-RAY BURST SPECTROMETER ON THE SOLAR MAXIMUM MISSION

L. E. Orwig, K. J. Frost and B. R. Dennis
Laboratory for Astronomy and Solar Physics
NASA-Goddard Space Flight Center
Greenbelt, MD 20771

August 1979

GODDARD SPACE FLIGHT CENTER
Greenbelt, Maryland

THE HARD X-RAY BURST SPECTROMETER ON THE SOLAR MAXIMUM MISSION

L. E. Orwig, K. J. Frost and B. R. Dennis
Laboratory for Astronomy and Solar Physics
NASA-Goddard Space Flight Center
Greenbelt, MD 20771

ABSTRACT

The Hard X-Ray Burst Spectrometer (HXRBS) to be flown on the Solar Maximum Mission is described. The primary scientific objectives of this instrument are as follows:

(i) To determine the nature of the mechanisms which accelerate electrons to 20-100keV in the first stage of a solar flare and to > 1MeV in the second stage of many flares;

(ii) To characterize the spatial and temporal relation between electron acceleration, storage and energy loss throughout a solar flare;

(iii) To search for previously undetected steady fluxes of solar X-rays; and

(iv) To measure any other solar X-ray phenomena in the unexplored time domain below 1s.

The observational objective is the measurement of the spectrum of solar X-rays in the energy range from 20 to 200keV with finer time resolution than has previously been possible. The X-ray detector designed to make these observations is an actively-shielded CsI(Na) crystal with a thickness of 0.635cm and a sensitive area of 71 cm^2. Continuous measurements with a time resolution of 0.128s will be made of the 15-channel energy-loss spectrum of events in this crystal in anticoincidence with events in the CsI(Na) shield crystal.

Counting rate data with a time resolution as short as 1ms will also be available for a limited period each orbit. This high time resolution data will consist of the number of counts detected each millisecond in a single channel covering the full energy range of the instrument, and will be stored in a 32K-word circulating memory for later, nighttime readout. The memory data will

cover a period from 13s before to 20s after a flare trigger event; longer accumulation periods are selectable with correspondingly poorer time resolution.

The sensitivity of the instrument is such that flares producing a 20-260keV X-ray flux of 2×10^{-1} photons/(cm^2 s) for one second will be just detectable. It is expected that ~1000 flares this large or larger will be detected in the first year after launch.

CONTENTS

ILLUSTRATIONS

THE HARD X-RAY BURST SPECTROMETER ON THE SOLAR MAXIMUM MISSION

SCIENTIFIC OBJECTIVES

The general scientific objective of the Hard X-Ray Burst Spectrometer (HXRBS) is to determine the role that energetic electrons play in the solar flare mechanism. The 20 to 260 keV bremsstrahlung generated by flare electrons as they lose energy in the solar atmosphere will be measured by the HXRBS to obtain information on the spectral and temporal history of these energetic electrons.

Impulsive X-ray emission, indicative of the first stage of electron acceleration (Frost and Dennis, 1971) will be measured in 15 channels covering the energy range from 20 to 260 keV with a time resolution of 0.1 second. The fine time structure of the impulsive X-rays in one energy channel from 20 to 260 keV will also be obtained simultaneously with the spectral measurements. The time resolution for these observations is programmable and may be selected to be as fine as one millisecond. The absolute timing accuracy of the spectral and high time resolution data will be one millisecond. This millisecond time resolution and absolute timing accuracy will afford us the opportunity to search for time-of-flight effects by measuring time differences between hard X-ray emission and other highly correlated emissions originating at different heights in a flare; e.g., microwave or type II meter-wave emission in the radio range. Bai (1978) has recently claimed that time resolution of one millisecond in hard X-ray observations may permit the determination of the source height and anisotropy of the hard X-ray emission.

A second type of X-ray emission occurring in some flares is indicative of acceleration of electrons to relativistic energies. This "second stage" X-ray burst occurs immediately after the impulsive X-rays, microwaves and type III bursts, and is coincident with type II and type IV bursts. The X-ray spectral, temporal and intensity characteristics are quite different from the impulsive X-ray stage. The spectrum is a power law with index from -2 to -6, the rise time is

10's of seconds, the decay time is minutes to 10's of minutes, and the duration may be as long as an hour. The location of the source is also likely to be different from that of the impulsive X-ray emission and may, in fact, be in the corona (Hudson, Ap. J. 224, 235, 1978).

The large area (71 cm^2), low background and steady solar viewing of the HXRBS will permit detection of second-stage X-ray bursts at a lower intensity and for a longer time than was previously possible. The HXRBS will, thus, provide a wealth of data on this relatively new component of hard X-ray emission.

DETECTOR DESCRIPTION

The Hard X-Ray Burst Spectrometer (HXRBS) on SMM is a collimated X-ray spectrometer similar to the types previously flown by this group on OAO-A, OSO-2, OSO-5 (Frost, et al., 1971), and OSO-8 (Dennis, et al., 1977). The detector portion of the instrument is very similar to the OSO-5 detector, differing only in the central detector and charged-particle detector designs and the addition of calibration light pulsers to the shield collimator. A cross-sectional view of the HXRBS detector is shown in Figure 1. The detector consists of two primary scintillation crystal components, a disk-shaped CsI(Na) central detector element and a CsI(Na) active collimator element which surrounds the central detector. Each of these two crystals is viewed by four photomultiplier tubes which convert the scintillation light pulses to electrical signals. The central crystal unit is the solar viewing detector, while the shield crystal serves as an X-ray collimator by providing for efficient X- and gamma-ray attenuation from non-solar directions as well as rejection of charged particle background events.

In addition to the main X-ray detector, the instrument also contains a charged-particle detector (not shown in Figure 1) consisting of a 2.5 cm diameter x 1.3 cm thick cylinder of Pilot B plastic scintillator viewed by a 2.5 cm diameter photomultiplier. This detector will monitor the flux of charged particles in the satellite orbit and will be used to automatically turn off the high voltages to the detector photomultipliers during passages through the South Atlantic Anomaly.

The 0.635cm thick central crystal has a sensitive area of 71 cm^2. The collimator geometry provides a field of view of 40° FWHM with a geometric area-times-solid-angle factor of 34 cm^2 ster. The measured energy resolution is 30% FWHM at 122keV. The total detection efficiency for X-rays incident parallel to the collimator axis is qualitatively the same as that of the OSO-5 instrument (see Frost, et al., 1971). There is a rapid decrease in total photon detection efficiency below 30keV due to attenuation in 0.14 gcm^{-2} of aluminum material over the central crystal and also by a 50 micron dead layer (Goodman, 1976) on the surface of the central crystal. The relatively thick aluminum windows were included to attenuate the large fluxes of soft solar-flare X-rays which would distort the measured X-ray spectrum above 20keV due to pulse pile-up effects. The reduced efficiency for detecting photons above 100keV is due to the decreasing interaction probability for such X-rays in the thin central crystal.

In-flight energy calibration of the central detector is achieved by the detection of 59.6keV X-rays emitted by an Am^{241} radioactive source embedded in a plastic scintillator button located in the detector field-of-view (see Figure 1). The Am^{241} isotope decays by the simultaneous emission of a 60keV X-ray and a 5MeV alpha particle. The alpha particle loses all of its energy in the button giving a large light pulse detected by the attached photomultiplier producing a calibrate event tag. The 60keV X-rays which escape the button and interact in the central crystal are detected in coincidence with these calibrate tag signals. The amplitudes of these calibrate events are recorded and used to generate a differential pulse-height spectrum to provide a continuous monitor of the detector energy calibration.

Central detector signals are operated in anticoincidence with the shield collimator signals. Therefore, fluctuations in the shield energy discriminator threshold level will significantly change the events being selected for pulse-height analysis. In-flight calibration of the shield discriminator threshold levels is obtained through the use of two Am^{241}/NaI(Tℓ) light pulsers (Harshaw Chemical Co.) inserted in the collimator crystal walls. Each pulser consists of Am^{241} radioactive source material embedded within a NaI(Tℓ) crystal. Alpha particles resulting from the decay of the Am^{241}

lose their energy in the NaI(Tℓ) and produce large light flashes which are detected by the collimator shield photomultipliers producing shield calibration events. An integral spectrum of these calibration pulser events plus normal shield events is repeatedly accumulated. The location of light pulser events in these spectra permit the shield anticoincidence energy threshold levels to be determined throughout the mission.

All detector components and system electronics are mounted on a single instrument baseplate, which is attached to the SMM Instrument Support Plate via a three-point mounting system. The instrument weighs 44.1 kg of which 15.9 kg are detector crystal components, occupies a volume 36.9 cm W x 83.9 cm L x 30.3 cm H, and requires 7 watts of primary power independent of spacecraft day or night.

DATA COLLECTION AND ELECTRONICS

One of the design criteria for the instrument was the desire to measure, without spectral distortion, an input differential photon spectrum with a power-law spectral index of -1.7 which would produce a counting rate in the detector of 10^5 counts/s. A flare producing such a spectrum would be a factor of ~2 more intense than the biggest flare ever observed, the flare of August 4, 1972. This criterion had a major impact on the data collection strategy and the detailed instrument electronics design discussed below.

Signals from the central crystal are operated in anticoincidence with signals from the shield collimator. Events of interest are, therefore, those in which there exists a signal in the central detector without a coincident signal in the shield crystal. A functional block diagram of the complete electronics which selects these events and performs the various data gathering tasks is shown in Figure 2.

The instrument produces a number of types of data from these selected events, as follows:

1. A fifteen-channel energy-loss spectrum between 20 and 260 keV in the central crystal is generated once every 128 ms. These spectra constitute the prime scientific data from the

instrument. Events of interest are pulse height analyzed into fifteen bins. Fifteen scalars are used to accumulate individual channel counts during each spectrum sample interval. The channel scalar capacities were sized to meet the intensity and spectral shape criteria stated above. The individual measured energy channel edges for the nominal energy range and channel scalar capacities are indicated below:

Channel No.	Channel Energy (keV)	Channel Scalar Capacity
1	Lower Threshold - 20	65536
2	20 - 34	65536
3	34 - 49	65536
4	49 - 64	4096
5	64 - 79	4096
6	79 - 93	4096
7	93 - 108	4096
8	108 - 123	1024
9	123 - 138	1024
10	138 - 152	1024
11	152 - 167	1024
12	167 - 182	1024
13	182 - 196	1024
14	196 - 211	1024
15	211 - 255	1024

A total of 22 8-bit telemetry words are used to read out this data into the spacecraft telemetry every 128 ms.

2. The second important set of data required to compute the incident photon spectrum is the total instrument live time. It is recorded for the same 128 ms interval over which the

event counts are accumulated. It is obtained by counting 500 kHz clock pulses during periods when the instrument is capable of detecting an acceptable event and is recorded to a precision of 0.128 ms. This live-time data is used to correct each energy-loss spectrum for instrument dead time. It is important that this correction factor has the same time resolution as the spectrum data being corrected and is therefore an accurate way of making this crucial instrument live-time correction. To encode the live-time data into telemetry requires 10 bits per 128 ms.

3. A third set of data is the central crystal Am^{241} calibration data, which permits constant monitoring of the stability of the entire central detector and pulse-handling electronics. As discussed earlier, X-ray events in the central crystal that occur in time coincidence with events in the alpha-particle calibration detector are tagged as calibration events. These events are pulse-height analyzed using the same electronics as for all central detector events. The amplitude of the last calibration event occurring during a 128 ms spectrum sample interval is stored and included in the telemetry. Accumulation of these calibration-event amplitudes over a period of time produces a 15-channel differential spectrum of the detector response to 59.6 keV X-rays and permits the stability of the central detector and pulse-handling electronics to be monitored.

4. In parallel with the accumulation of 15-channel spectral data the instrument also provides high time resolution counts-vs.-time data through use of a large 32768-byte solid-state memory operated in a continuously circulating manner (see Figure 2). This memory has four basic operating modes which will be discussed briefly in the next section. The memory data contain no energy spectrum information, but give the total count of events in one large energy window which occur during each memory sample interval. It is capable of storing event counts vs. time down to a time resolution of 1 ms. Its purpose is to explore solar X-ray flare emission fluctuations with high time resolution.

In the principal mode of operation, the memory continuously counts and stores the number of input events occurring during consecutive memory sample intervals. Each count sample becomes one byte of data in the memory. The memory continually stores this data, always over-writing the oldest data, until it receives an event trigger flag internally generated within the instrument. A trigger flag is generated when the count in any one of three counters exceeds independently selectable thresholds. These scalars have count integration times of 4ms, 32ms, and 256ms. Upon receipt of this flag the memory will store 19456 more count samples, be declared full, and await readout to telemetry. In this way the memory stores 32768 contiguous samples of data, 13312 of which are pre-trigger, and 19456 post-trigger. The total time required to fill the memory is a function of the length of each individual memory sample interval. This interval can be configured in flight from 1 ms to 255ms per sample in 1 ms increments. Control of the entire memory requires two pulse commands and one 16-bit serial magnitude command. Information on the detailed memory configuration and present state of the memory is included in the general housekeeping data.

In addition to the principal data listed above, housekeeping data is also recorded on a much slower time scale. This data includes information on command and instrument status, fourteen analog voltages, and two temperatures, all recorded once every 8.192s. Further data includes the counts above certain threshold levels in various detector components sampled over a 16.384s time interval. Since the variation in count rate above a threshold level is a good measure of the stability of that level, this data provides for sensitive monitoring of these energy thresholds. Also, 64-channel integral spectra of events in the central detector and shield collimator are accumulated once every 64 telemetry major frames (524s). These spectra are obtained by sampling the number of events which exceed an energy threshold each major frame. This threshold is then stepped through 64 levels, once every 8.192s, thereby generating the desired integral spectra. This process is then repeated for a new spectrum.

One of the principal design criteria for the instrument electronics was the desire to produce pulse height spectra at average total data rates of 10^5 counts/s. with minimum spectral distortion. To this end all central detector shaping amplifiers utilize bipolar RC shaping with total pulse widths of $6\mu s$. Such amplifiers minimize baseline shifts and pulse pile-up, the two effects which distort the measured spectrum at high data rates. All preamplifiers and analog pulse amplifiers are modified versions of those used in our OSO-8 instrument (Dennis, et al., 1977). All digital pulse-handling circuitry was designed to operate at 5×10^5 counts/s peak rate with little or no degradation in performance. Coincidence resolving times are kept at $\leq 1\,\mu s$ to improve the rate handling capabilities of the instrument and optimize any distortion in the pulse height analyzer due to pulse jitter.

To determine the instrument response to a fixed X-ray spectrum over a wide range of event counting rates, spectra were recorded from a 3.3 mC Sr^{90} source positioned at various distances from the detector. This source produces an X-ray continuum over the energy range of interest. At each position an energy-loss spectrum was accumulated for an integration time of 160 s. The results for seven of these measurements are shown in Figure 3. The total rates shown on the figure are the final pulse-height analyzed event rates. For each run the instrument was handling total pulse rates which were at least 50% higher than the indicated rate. At the highest counting rates the spectrum becomes flatter. This distortion amounts to a 17% change in the spectral index of the exponential fit to the high-energy tail of the distribution for the 1.1×10^5 counts/s data. The data points with error bars are the result of a single 128 ms accumulation while sweeping the source through the detector field-of-view to simulate rapid count-rate fluctuations. The fit of the above curve to this data is within the statistical fluctuations. Although X-rays with a spectrum much harder than that expected from solar flares were used in this test, the measured energy-loss spectra clearly demonstrate the instrument capabilities at high rates.

An indicated in Figure 2, individual central-detector phototube signals are amplified in variable-gain amplifiers and then linearly added prior to being selected for pulse-height analysis.

The individual photomultiplier amplifier gains are commandable and are chosen to recover nominal instrument operation in case of a failure of one or more photomultipliers, or a failure of either of the two high voltage power supplies. The discriminator threshold level for nearly every detector component is adjustable in a number of commandable steps. These will be adjusted in flight to optimize instrument performance. With both high voltage supplies and all photomultipliers operating nominally, a choice of eight central detector pulse height energy ranges exists, varying from 7-113keV to 49-840keV. Within each of these ranges the lower threshold level is adjustable in 4 steps. The shield anticoincidence threshold level is adjustable in 8 steps from 46keV to 680keV. The lower threshold level for the central calibration detector is adjustable in 4 steps, and the charged-particle detector discriminator threshold level can be adjusted in 4 steps from ~200keV to ~1100keV.

OPERATIONAL MODES

The instrument has two main data collection modes, the continuous accumulation of energy-loss spectra with 128ms time resolution and the accumulation of counts-vs.-time data in the large circulating memory with high time resolution but with no spectral information. The operational mode for accumulating spectral data is fixed. The memory has four basic data gathering modes and its readout into telemetry can be affected in several ways. Due to this flexibility, the operational modes of the memory must be optimized to gather the maximum amount of scientific data from the mission. In this regard, however, it must be remembered that this memory is an exploratory data gathering device and the information it generates is not the prime scientific data. Although the final determination of optimum operating modes for this memory will have to await the results of its initial performance in the early phase of the mission, several possible modes of operation are envisioned at the present time.

The burst memory can sample incoming event signals in two ways: (i) it can store the number of events occurring during a selected constant sample time interval (constant time, CT, mode), giving 32768 such samples, (ii) or it can store the amount of time (number of clock pulses

of a 16kHz clock) required to count a selected number of events (constant count, CC, sample mode). In the CT mode the individual sample time is commandable from 1 to 256ms, and in the CC mode the individual sample count is adjustable from 1 to 256 counts per sample. In either of these modes the input data being counted can be either events from the central detector (CD events) or events from the shield (SH events). Consequently, there are four basic data collection modes for the memory: it can be operated in the CT mode counting either CD or SH events, or in the CC mode counting either CD or SH events.

In the CT mode of operation the total time required to fill the memory is purely a function of the selected sample interval and can vary from ~33s to ~140 minutes. In the CC mode the memory fill time is a function of the input data event rate but electronics' limitations impose minimum and maximum fill times of 1 second and 140 minutes respectively.

Readout of the memory contents to telemetry can be achieved in several ways: (i) a command from the ground can immediately initiate a memory dump whether the memory is considered full or not, (ii) the memory can be configured to automatically read out when declared full without ground command, or (iii) it can be configured to be automatically read out only if declared full and the spacecraft is in a night portion of the orbit. In all cases a memory dump to telemetry will preempt recording of the prime energy-loss spectral data since it utilizes the readout envelopes and clocks normally reserved for spectral information. Each memory dump requires 22 telemetry major frames (~180 seconds) to complete. Upon completion of a dump sequence, the telemetry is returned to the readout of the spectral data, and the memory is reinitialized and begins sampling automatically. Since a memory dump does preempt prime instrument data, the choices of sampling mode, adjustable parameter selection, and readout mode must be made very carefully to prevent any undue loss of spectral data.

It is expected that during the early phase of the mission the following operational modes for the memory will be utilized:

1. During spacecraft day the memory will be configured in the CT sample mode counting central detector events with an individual sample time of ~10ms. Memory trigger flag thresholds will be set at least 4σ above normal instrument background to prevent accidental triggering. Memory readout will be permitted to occur automatically only during spacecraft night. This memory mode will initially be used as the basic exploratory monitor of solar X-ray flare emission and will yield a maximum of one 328s snapshot with 10ms time resolution of any flare which initiates a memory trigger flag. Nighttime readout will assure that prime spectral data is obtained during the entire day portion of every orbit.

2. Initial orbit night operation will place the memory in a CC sampling mode with shield events as the input data to the memory. Memory readout to telemetry will be permitted only if the memory is triggered and becomes full during spacecraft night. The sample count interval and trigger thresholds will also be changed to accommodate the higher shield event rates. This mode will be used as a gamma-ray burst monitor during spacecraft night to search for non-solar gamma-ray burst phenomena. The shield is used as the non-solar burst detector because of its larger area and greater detection efficiency for higher energy X-rays and gamma-rays compared to the central detector. In addition it is an omnidirectional detector and hence is sensitive to gamma-ray bursts from all directions not occulted by the earth.

Based on the early in-orbit performance of this circulating memory its' operating modes will be adjusted to optimize the collection of data for specific scientific objectives.

EXPECTED PERFORMANCE

The sensitivity of the HXRBS to solar X-ray fluxes depends on the total background counting rate of the instrument and the ability to detect increases in rate above this level. The background spectrum has been studied in some detail for the similar instrument flown on OSO-5 in essentially the same orbit as that planned for SMM (Dennis, et al., 1973).

The detector background is made up of two basic components:

– counts resulting form the diffuse component of the cosmic X-ray flux, and

– counts resulting from the decay of the induced radioactivity of the CsI(Na) crystal produced as the satellite passes through the high proton fluxes of the inner radiation belt in the region of the South Atlantic Anomaly.

The resulting background spectrum, as determined from the OSO-5 data, builds up in the first weeks after launch to a steady average daily level as an equilibrium is reached between the production and decay of the long-lived radioactive isotopes. A daily variation by a factor of 2 to 4 also occurs as a result of the decay of the short-lived isotopes after each passage through the South Atlantic Anomaly. An accurate measure of the background level during a flare can be obtained by using the data immediately preceeding and following the flare. This technique allows even the weakest flares above the instrument sensitivity level to be reliably detected.

We have computed the sensitivity of the HXRBS to solar flare X-rays using an average background counting rate in the energy range from 30–200 keV of 10 counts/s as observed on OSO-5. A plot of this sensitivity for a range of integration times is shown in Figure 4. We have assumed that all fluctuations in the background counting rate are statistical and that an increase in the rate by three standard deviations is required to constitute a positive detection of solar X-rays. At integration times of less than approximately 30 ms the expected number of background counts becomes less than one, so we have assumed that at least three counts are required from the flare to constitute a significant observation. The resulting curve showing the minimum detectable flux above background for the HXRBS is approximately a factor of three below the corresponding curves for the TD1A and OSO-5 instruments in the time domain above 1–2 s where they overlap. The HXRBS curve extends down to integration times as short as 1 ms and is significantly below the curve for the shield crystal of the balloon-borne X-ray detector flown by Hurley and Duprat (1977), which achieved millisecond time resolution for a solar flare detected in July 1974.

The number of flares which we expect to detect above our sensitivity threshold can most easily be determined by comparison with the rate of flares observed by the similar instrument on OSO-5 at the same phase of the previous solar cycle. Using this data and allowing for the factor of three increase in sensitivity of the HXRBS, we expect to be able to detect of the order of 1000 flares in the first year of operation after launch. The fraction of this number which will show variability on time scales of less than one second cannot be estimated, but, based on the flare observed by Hurley and Duprat (1977) and the radio observations of Slottje (1978), Dröge (1977), and Kaufman, et al., (1979), such rapid variability may not be a rare phenomenon. Consequently, we expect to collect data for many solar flares which will be highly relevant to achieving our scientific objectives.

ACKNOWLEDGMENTS

The HXRBS detector was built in the Laboratory for Astronomy and Solar Physics at Goddard Space Flight Center. We are indebted to the efforts of many people in this laboratory who worked on this project. In particular the authors wish to thank G. Dietz for detector mechanical design; R. Lencho for analog electronics design; T. Plummer and C. Nash for detector electronics fabrication; A. Huffman for photomultiplier and detector assembly; F. Hallberg for high voltage supply testing; C. Howell for programming support; D. Burritt for administration and purchasing; and B. Jackson, C. Clark, and W. MacDonald for secretarial support. Numerous people from other divisions at Goddard also contributed to the success of this effort: C. Cancro, H. White, L. Workman, J. Gillis, R. Baker, M. Peck, and W. Bush who designed and tested the subsystem electronics; J. Wolfgang who supervised the electronics engineering effort; and H. Becraft who did much of the electronics layout.

Finally we wish to thank the personnel at a number of outside contractors for their fine performance; notably a task group from the CSC Corporation for programming the ground support equipment, Ideas Inc. for the analog and digital electronic packaging design and fabrication, the Harshaw Chemical Company for the CsI(Na) crystals, and Mega Engineering for the design and fabrication of the instrument baseplate.

REFERENCES

Bai, T.: 1978, Solar Physics, 59, 141.

van Beek, H. F.: 1973, "Development and Performance of a Solar Hard X-Ray Spectrometer," Utrecht University (Ph.D. Thesis).

Datlowe, D. W., Elcan, M. J., and Hudson, H.S.: 1974, Solar Physics, 39, 155.

Dennis, B. R., Frost, K. J., Lencho, R. J. and Orwig, L. E.: 1977, Space Science Instrumentation, 3, 325.

Dennis, B. R., Suri, A. N. and Frost, K. J.: 1973, Ap. J., 186, 97.

Dröge, F.: 1977, Astronomy and Astrophysics, 57, 285.

Frost, K. J. and Dennis, B. R.: 1971: Ap. J., 165, 655.

Frost, K. J., Dennis, B. R., and Lencho, R. J.: 1971, "New Techniques in Astronomy," I.A.U. Symp., 41, 185.

Frost, K. J., and Rothe, E.: 1962, IRE Trans. Nucl. Sci., (Proc. 8th Scintillator Counter Symp.), NS-9, 3, 381.

Goodman, N. B.: 1976, Space Science Instrumentation, 2, 425.

Hudson, H.S.: 1978, Ap. J., 224, 235.

Hurley, K. and Duprat, G.: 1977, Solar Physics, 52, 107.

Kaufman, P., Strauss, F. M., Opher, R., and Laporte, C.: 1979, Astron. Astrophys., in press.

Slottje, C.: 1978, Nature, 275, 520.

FIGURE CAPTIONS

Figure 1. Cross-sectional view of the Hard X-ray Burst Spectrometer.

Figure 2. Simplified functional block diagram.

Figure 3. Differential count rate spectra obtained with a 3.3 mC Sr^{90} source placed at different distances from the detector to show the effect of high count rates on the spectral shape. The smooth curve through each set of points is the curve fitted through the 1.2×10^4 counts/second data multiplied by a constant factor to best fit the data at other total rates. The difference between each curve and the corresponding set of data points is a measure of the effects of the total counting rate on the observed spectral shape. The data points with ±1 sigma error bars were obtained in a 128 ms interval when the Sr^{90} source was moved rapidly across the detector aperture, a test designed to simulate short-term fluctuations in rate. The total duration of the burst from the Sr^{90} source was ~0.3 s.

Figure 4. The minimum detectable X-ray flux above the detector background in the energy range from 30 to 200 keV as a function of the integration time. The normal-mode data will cover integration times down to 128 ms. The memory data will be available for a limited time each orbit as explained in the text and will cover integration times down to 1 ms. Curves for the high energy X-ray detectors on OSO-5 (Frost, et al., 1971), TD1A (van Beek, 1973), OSO-7 (Daltowe, et al., 1974) and the balloon instrument flown by Hurley and Duprat (1977) are shown for comparison.

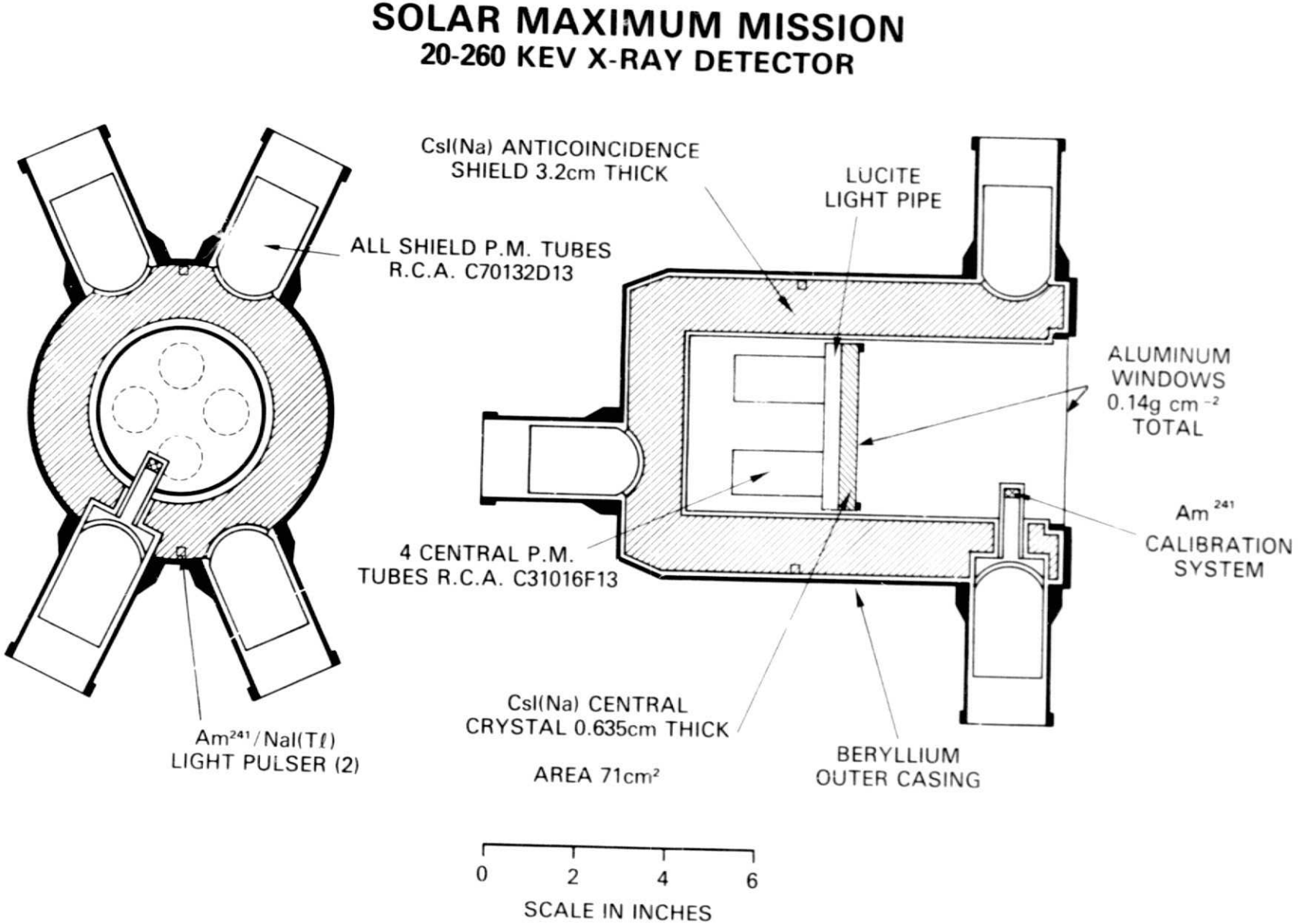

Figure 1. Cross-sectional view of the Hard X-Ray Burst Spectrometer.

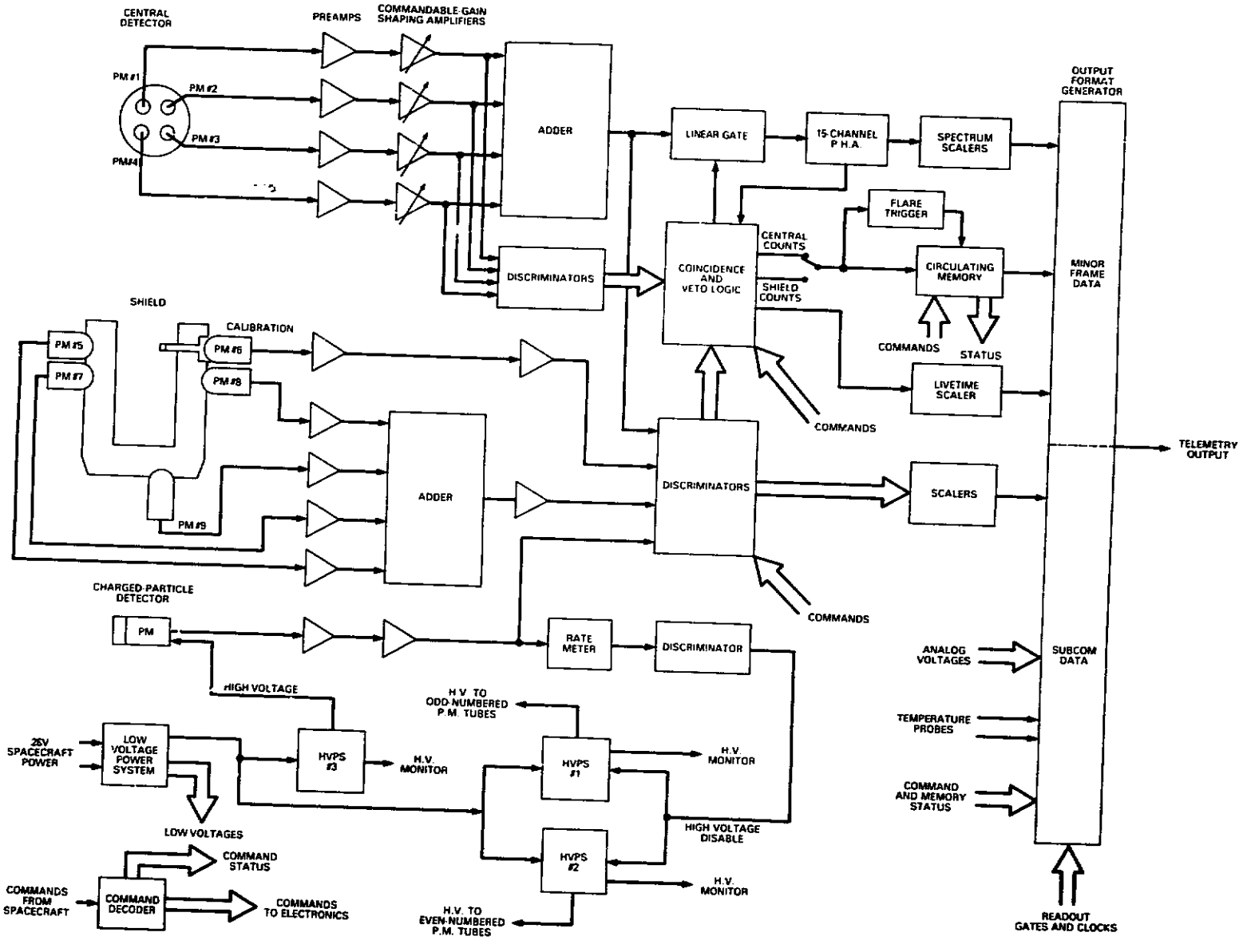

Figure 2. Simplified functional block diagram.

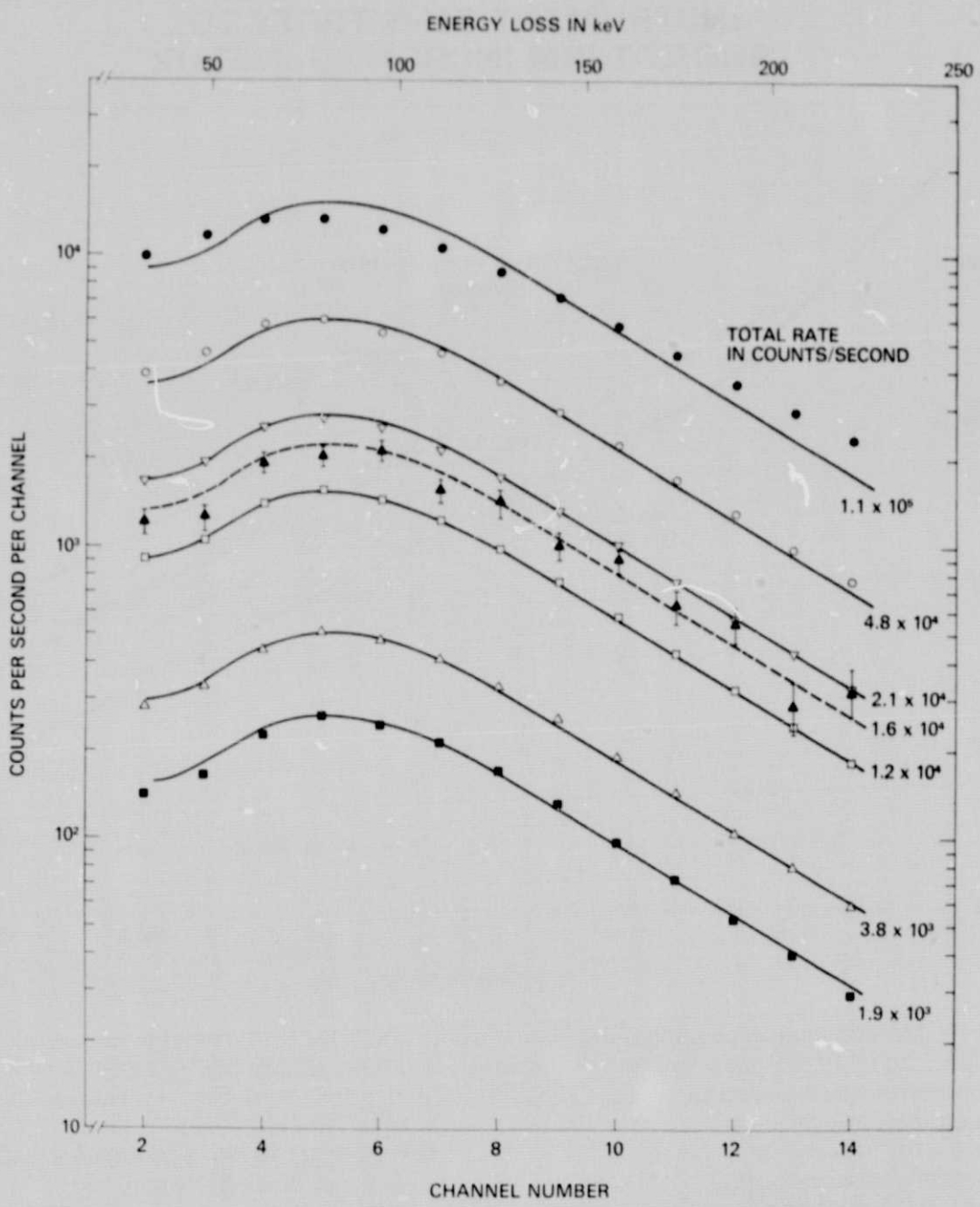

Figure 3. Differential count rate spectra obtained with a 3.3 mC Sr^{90} source placed at different distances from the detector to show the effect of high count rates on the spectral shape. The smooth curve through each set of points is the curve fitted through the 1.2 x 10^4 counts/second data multiplied by a constant factor to best fit the data at other total rates. The difference between each curve and the corresponding set of data points is a measure of the effects of the total counting rate on the observed spectral shape. The data points with ±1 sigma error bars were obtained in a 128 ms interval when the Sr^{90} source was moved rapidly across the detector aperture, a test designed to simulate short-term fluctuations in rate. The total duration of the burst from the Sr^{90} source was ~0.3 s.

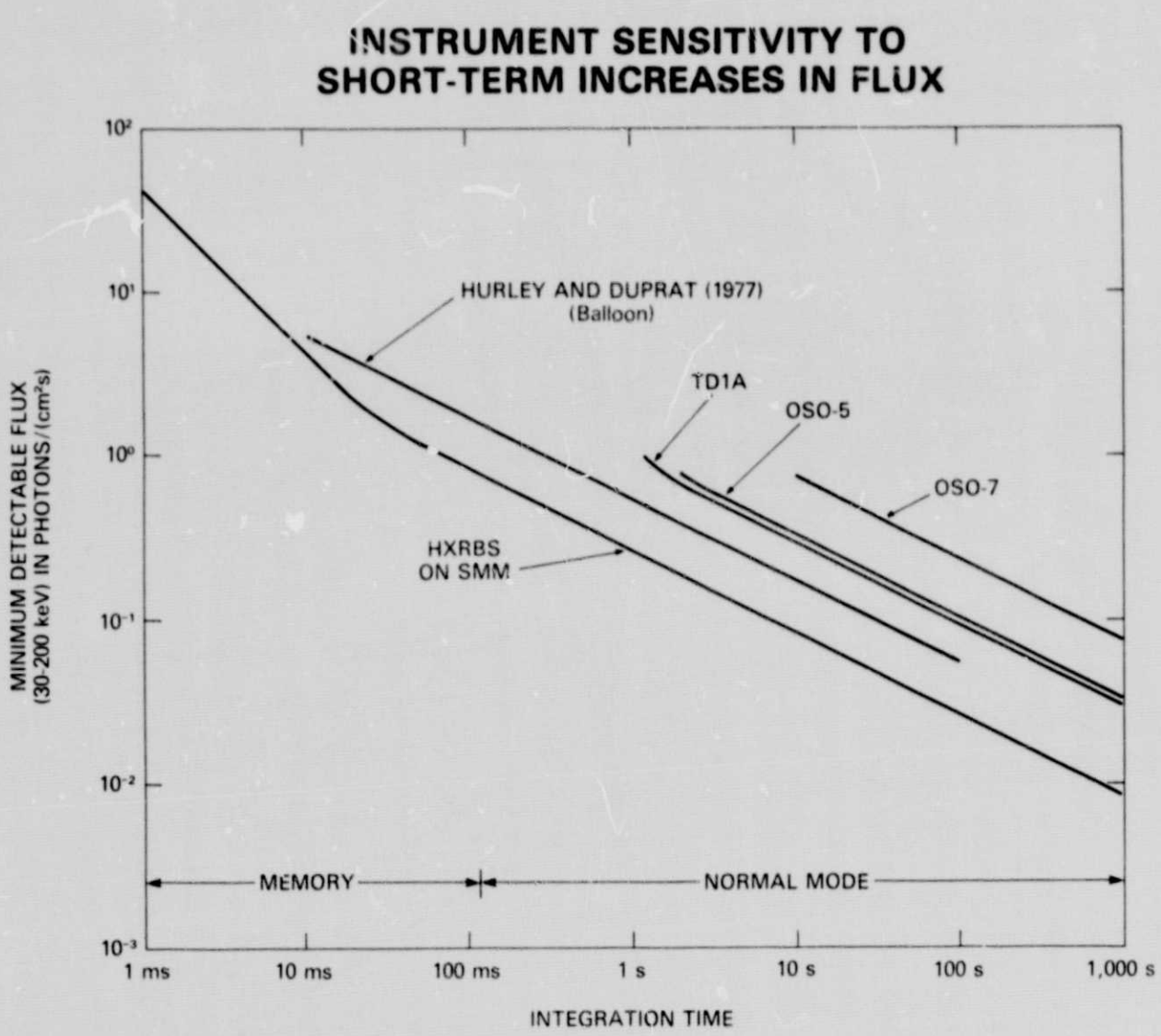

Figure 4. The minimum detectable X-ray flux above the detector background in the energy range from 30 to 200 keV as a function of the integration time. The normal-mode data will cover integration times down to 128 ms. The memory data will be available for a limited time each orbit as explained in the text and will cover integration times down to 1 ms. Curves for the high energy X-ray detectors on OSO-5 (Frost, et al., 1971), TD1A (van Beek, 1973), OSO-7 (Daltowe, et al., 1974) and the balloon instrument flown by Hurley and Duprat (1977) are shown for comparison.